Knowledge-Based IMRT Treatment Planning for Prostate Cancer: Experience with 101 Cases from Duke Clinic

by

Deon Martina Dick

Department of Medical Physics
Duke University

Date:_____
Approved:

_____
Joseph Lo, Chair

_____
Shiva Das, Chair

_____
Robert Reiman

Thesis submitted in partial fulfillment of
the requirements for the degree of Master of Science in the Department of
Medical Physics in the Graduate School
of Duke University

2012

ABSTRACT

Knowledge-Based IMRT Treatment Planning for Prostate Cancer: Experience with 101 Cases from Duke Clinic

by

Deon Martina Dick

Department of Medical Physics
Duke University

Date:_____
Approved:

_____
Joseph Lo, Chair

_____
Shiva Das, Chair

_____
Robert Reiman

An abstract of a thesis submitted in partial fulfillment of the requirements for the degree of Master of Science in the Department of Medical Physics in the Graduate School of Duke University

2012

Abstract

Intensity-modulated radiotherapy (IMRT) has become an effective tool for cancer treatment with radiation. However, even expert radiation planners still need to spend a substantial amount of time, approximately 4 hours, manually adjusting IMRT optimization parameters such as dose limits and costlet weights in order to obtain a clinically acceptable plan[2]. Also, the quality of the treatment plan generated is solely based on the experience and training of the planning. In comparing the geometries of the planning target volume (PTV), bladder, rectum, right and left femoral heads, a knowledge-based approach to IMRT treatment planning may reduce the time needed to generate a clinically acceptable prostate plan. The knowledge-based approach uses the clinically acceptable plans of previously irradiated patients which are adapted to the new patient. Patient selection is done by using mutual information (MI). Having selected the best matched patient, Elastix (a toolkit for rigid and deformable registration) is used to deform the treatment plan of the previously irradiated patient to the new patient's geometry. The Eclipse treatment planning system is used to generate both pre-optimized and post optimized plans for the new patients. The knowledge-based treatment plans require no manual intervention. For the 101 patient data, it was shown that the newly generated plans were of similar or slightly worse dosimetric quality and were only generated in less than 30 minutes. Given the large size of this data set, the results are likely to be robust in representing treatment planning efficacy over a diverse

range of patient anatomy. This work has the potential to automatically provide high quality treatment plans while dramatically reducing the dependence of the expertise of the planner and the treatment planning time.

Contents

List of Tables

List of Figures

Acknowledgements

I would like the thank Dr. Joseph Lo and Dr. Shiva Das for being my advisors throughout this research and Dr. Reiman for serving as a part of my committee.

I would also like to thank my parents, Rev. Dr. Devon and Mary Dick for not only financially supporting me throughout my tenure at Duke University, but for the encouragement on those days that looked bleek.

David Good and Christopher Busselburg were also helpful in fostering a great research environment where we picked apart each other's' brains to enhance our respective research interests. Three heads are always better than one.

This research was supported in part by a seed grant from the Duke Cancer Institute, the Summer Scholarship Program of the Duke Graduate Program in Medical Physics, the National Health Fund (NHF) in Jamaica, West Indies and the Culture Health Arts Sports and Education fund (CHASE) also based in Jamaica, West Indies.

1. Introduction

Prostate cancer is the second leading form of cancer related deaths among American men, behind lung cancer. According to the American Cancer Society, 1 in 36 American men will die of prostate cancer[1]. It is estimated that 241,750 men will be diagnosed with prostate cancer in 2012 which is 850 more men estimated in 2011[2]. There are different techniques that are used to treat prostate cancer using external beam radiation therapy (EBRT), including Helical Tomotherapy, RapidArc Therapy, Intensity-Modulated Radiotherapy (IMRT) and 3D Conformal Therapy.

RapidArc therapy has proven to be an effective tool in treating prostate cancer as it minimizes the dose to the organs at risk (OAR). However, this technique does not deliver a therapeutic dose to the tumor[3-5]. TomoTherapy is also effective in treating prostate cancer as the dose to the organs at risk is minimized and the tumor dose is therapeutic[6-9]. RapidArc, TomoTherapy and IMRT are all treatment techniques that produce a variety of treatment plan qualities but are all improvements to the 3D conformal radiation therapy[10-12]. The 3D conformal therapy is the least effective tool for treating prostate cancer as the dose to the OARs are not minimized and the dose coverage of the target tumor is the least therapeutic of the techniques mentioned above [13-15]. The treatment technique used in this study is IMRT.

IMRT is a conformal radiation technique that is used to minimize the dose to the organs-at-risk (OAR) and maximize the dose to the target tumor. This is accomplished

by changing the intensity of the radiation during treatment. IMRT is mainly used to treat the prostate, head and neck and central nervous system cancers and, in limited cases, the thyroid, breast and lung.[16] IMRT can be delivered using two methods: step and shoot and dynamic multi-leaf collimator which are equally effective at treating cancer[17-19]. Most prostate cancer patients undergo IMRT, which result in 90% disease-free rates after five years for early stage cases[20].

For the treatment of prostate cancer, the target is the prostate with a 0.5cm margin known as the planning target volume (PTV). The healthy organs that are at risk for receiving dose during the treatment are the rectum, bladder and the right and left femoral heads (see figure 1).

Figure 1: 3D image of the body with the PTV, bladder, rectum, left and right femoral heads

For the treatment of prostate cancer with IMRT, 5-9 angles are used to deliver a more therapeutic dose to the PTV and minimize the dose to the OARs. At the Duke Clinic,

seven (7) angles located at angles 25°, 75°, 130°, 180°, 230°, 280° and 335° are used to deliver a course of radiation as shown in figures 2 and 3 below.

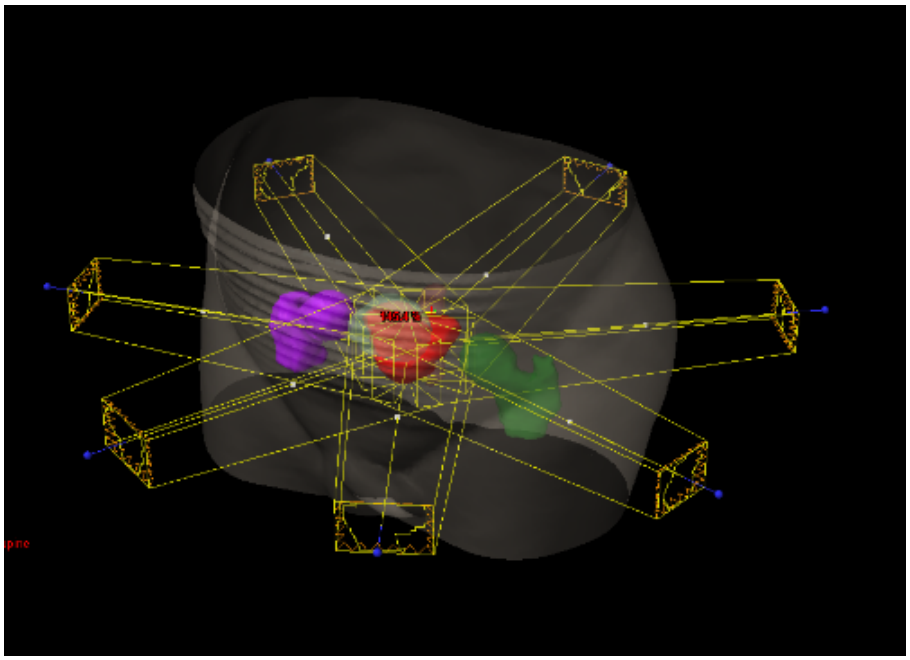

Figure 2: 3D image of pelvic anatomy of patient with the seven (7) treatment beams

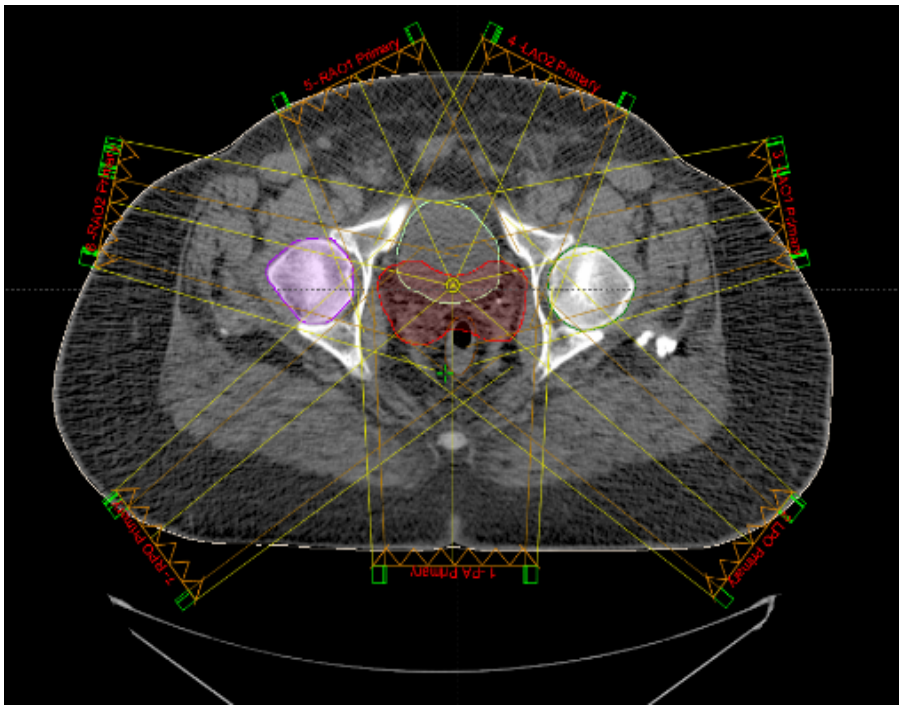

Figure 3: Axial slice of pelvic area with the seven (7) treatment beams

To obtain a clinically acceptable plan using IMRT, a trained medical physicist manually adjusts the IMRT optimization parameters. These parameters are the volume and dose constraints for the PTV and the OARs. The optimization parameters are subjective as they are dependent on the clinical experience of the radiation oncologist, and the relationship between dose and tissue complications are population-based and not well understood. The optimization process yields fluences which are maps of the beam intensity at each of the seven angles. To generate these fluences, a leaf-setting algorithm is used to determine the motion or the dynamic multileaf collimators. This algorithm uses techniques that minimize the total beam delivery time can be applied to the 'step-and-shoot' and 'dynamic' IMRT treatment delivery[21].

The quality of the treatment plans are determined from the isodose line distribution and dose volume histograms (DVH) generated from the optimization process. These methods of plan evaluation show the dose distribution throughout the anatomy of the patient. Figures 4 and 5 below are examples of the isodose line distribution and DVH curves.

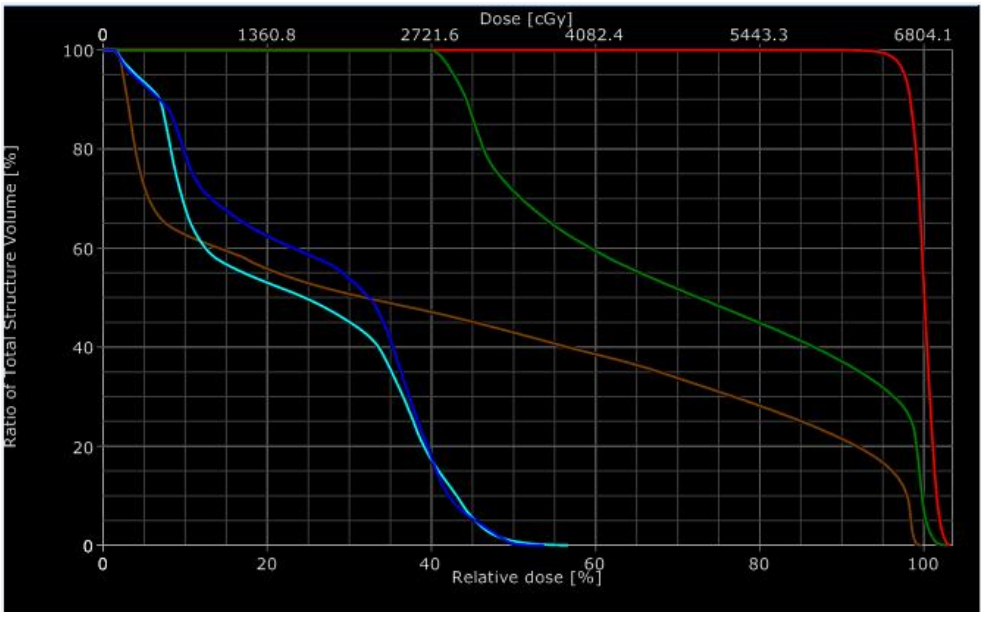

Figure 4: Example DVH of PTV (red), bladder (green), rectum(brown) right femoral head(blue) and left femoral head (cyan)

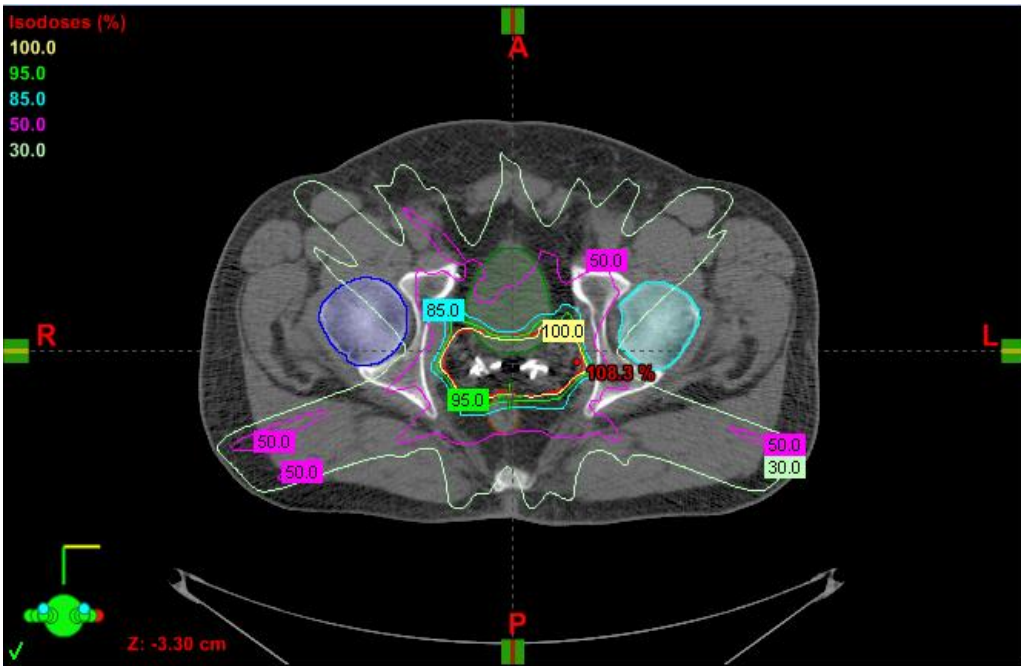

Figure 5: Axial CT Image of pelvic region with PTV(red), bladder (green), rectum (brown), right femoral head(blue) and left femoral head (cyan) and isodose lines

Though IMRT treatment plans are of high clinical quality, the time needed to manually adjust these parameters is substantial. The knowledge-based approach to IMRT treatment planning is a solution to reducing the time needed to generate a treatment plan of high dosimetric quality. Our previous group [22] developed an approach to knowledge-based IMRT treatment planning for prostate cancer, the model of which is used in this study.

The results previously reported by our group show that the treatment plans generated via the knowledge-based approach were of comparable or better dosimetric quality than the previous clinically acceptable plans. With 20 cases planned, however, this result has minimal statistical application. In addition, the methodology previously

offered by our group was primarily based on the user's discretion which led to each case being altered differently. In this study, 101 cases were planned, which significantly increases the statistical relevance of the data generated and the planner's involvement in the treatment planning process is considerably reduced.

2. Methods and Materials

2.1 Human Subject Data

For this study, a database of 150 prostate cancer patients who were treated using Intensity Modulated Radiotherapy (IMRT) was collected from the Duke University Radiation Oncology Department and anonymised. A Computational Environment for Radiotherapy Research (CERR) is used to convert the DICOM files extracted from the Eclipse treatment planning station into MATLAB (MathWorks, Natick, MA) files.

From the database, a query case is selected and acts as a new patient that needs a treatment plan. One hundred and one (101) cases were used as query cases and each case was compared to the other 149 cases in the database which are referred to as the match cases. The cases used in this study were all treated using seven beams (see Figure 6 below), the PTV did not includes nodes, the patient has no prosthetics and the match cases all had PTV dose-volume objectives.

The seven (7) beams used to deliver the IMRT radiation treatment plan are usually located at angles 25°, 75°, 130°, 180°, 230°, 280° and 335°. Using CERR, the 2D projections of each structure for each patient obtained at these seven standard angles are known as the beam's eye views (BEV). Masks, image with all the five structures, are created such that the isocenter, PTV, rectum, bladder, left and right femoral heads have pixel values of 32, 16, 8, 4, 2 and 1. An example of the masks at the seven angles are shown in Figure 6 below.

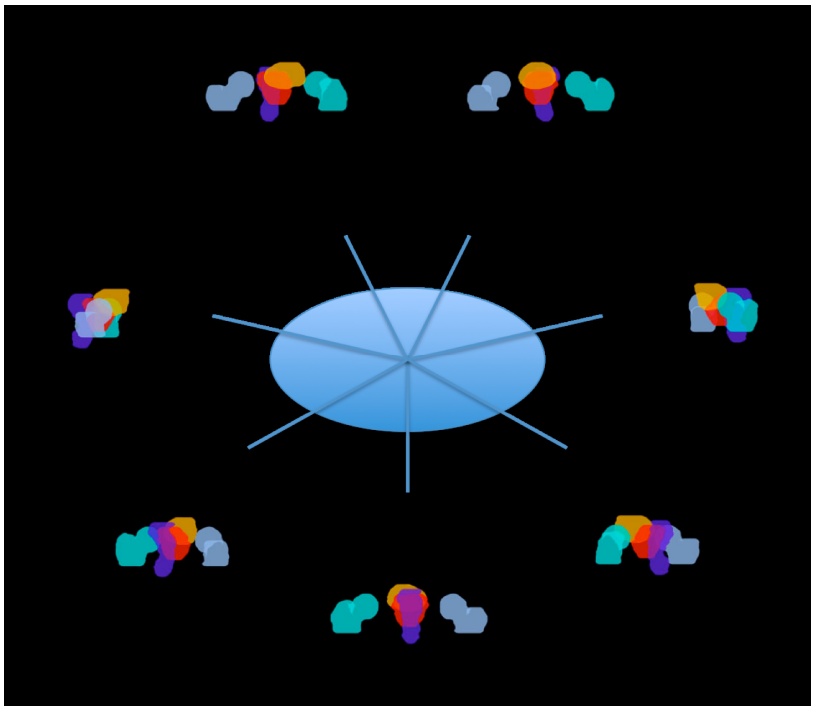

Figure 6: Figure showing masks at the seven standard angles

2.2 Determining the matches

The key to determining the similarity between the cases is the anatomy of the patients at the seven angles. The anatomy, displayed on the CT scans of the patient, can seem higher or lower in the BEVs projections depending on the cut points of the CT scan area. The CT scan area varied from patient to patient as shown in Figure 7 below.

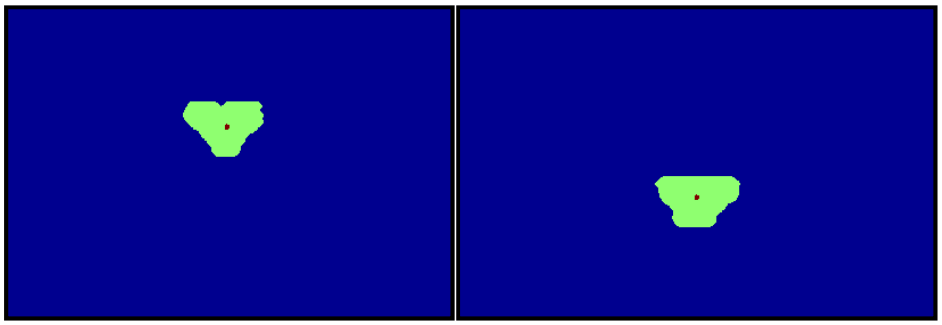

Figure 7: BEV image of PTV with a scan starting low in the body (left) and the other with the scan starting high in the body (right)

As a result, the masks were all centered such that the isocenter, indicated by the red dot in Figure 7, is located at the center of the 2D images; the shifts were made to the PTV and the OARs based on the position of the isocenter from the center of the image. (See Figure 8 below)

Figure 8: Mask showing that the PTV and OARS have been centered based on the isocenter location

All the masks for each of the 101 cases were modified as shown in Figure 8 above before applying the case-similarity algorithm. In order to determine the similarity between the BEVs obtained, mutual information (MI) is used. Mutual Information (MI) is a metric used in the knowledge-based methodology which measures the mutual dependence of two variables and is calculated as shown in Equation 1.

$$MI(A,B) = \sum_{i_a,i_b} P_{AB}(i_a,i_b) log_2 \left(\frac{P_{AB}(i_a,i_b)}{P_A(i_a)P_B(i_b)} \right)$$

where i_a is the intensity level in image A

i_b is the intensity level in image B

P_{AB} is the joint probability distribution function of image A and B

P_A is the marginal probability distribution function of image A

P_B is the marginal probability distribution function of image B

Each query case will have 150 MI values which represents how well each case in the database matches that query case. To quantify similarity between the query and match cases, mutual information (MI) values of the query vs. match masks are averaged over all the standard angles as shown in equation 2.

$$MI = \frac{MI1 + MI2\ MI3 + MI4 + MI5 + MI6 + MI7}{7}$$

where MI is the average of the MI values at the seven angles

The best matched case, indicated by the 2nd highest MI value for that query case, is selected in order to create a new plan for the query patient. The treatment angles of the best match case, determined by the highest MI value, are the angles used to create the BEV projections of the query and match PTV.

2.3 Deformation and Planning

Using the knowledge-based approach, a treatment plan is created by adapting the fluence of a previously irradiated patient to the new patient's anatomy. The deformation of the match's fluence is done using a toolbox for rigid and non-rigid registration known as Elastix (obtained under BSD, GNU and Open Source licenses) [23, 24]. Elastix has been used as a deformable registration toolbox for treatment sites such as the cervix[25] and other imaging modalities such as MRI[26, 27]. An important tool for using Elastix is the parameter file (see Appendix A). The parameter file is the key that tells Elastix the type of deformation, registration techniques among other parameters to successfully deform the images. Figure 9 below shows an example of the deformation of the fluence.

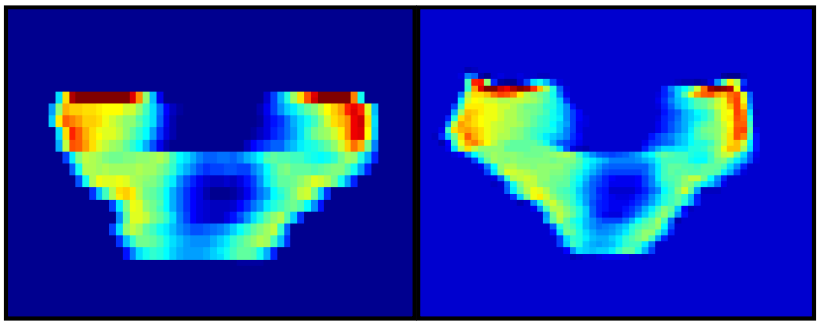

Figure 9: Figure of non-deformed fluence (left) and deformed fluence (right)

Before deforming the fluences, however, the PTV of the query and match cases are scaled and cropped to the dimensions of the match fluence. A deformation map, created when deforming the match PTV to the query PTV, is applied to the match's fluence for each of the seven angles. The dimension similarity is necessary for Elastix to deform the fluences appropriately. Figure 6 shows the BEV images before and after the cropping and scaling process. Figure 9 shows the dimensions of the match fluence.

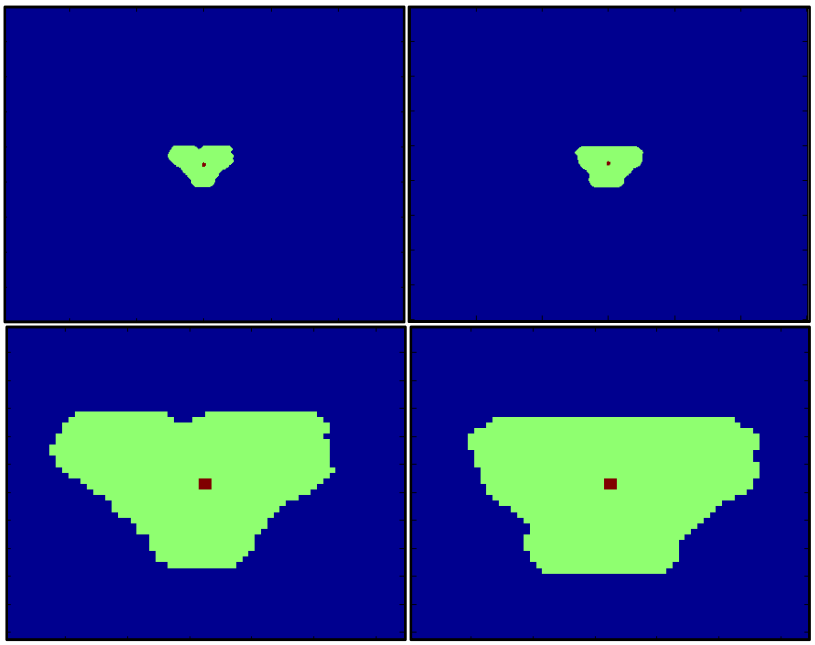

Figure 10: Query PTV before cropping and scaling (top and bottom left) and the match PTV after cropping (top and bottom right)

The deformed fluences (see figure 9) for each of the seven angles are then imported into the Eclipse treatment planning system (version A10, Varian Medical

Systems, Palo Alto, CA). The deformation process is essential to the knowledge-based planning methodology as the goal is to get the match fluence to have the shape of the query PTV. In Figure 11, the non-deformed match fluence super-imposed on the query PTV has the shape of the match PTV.

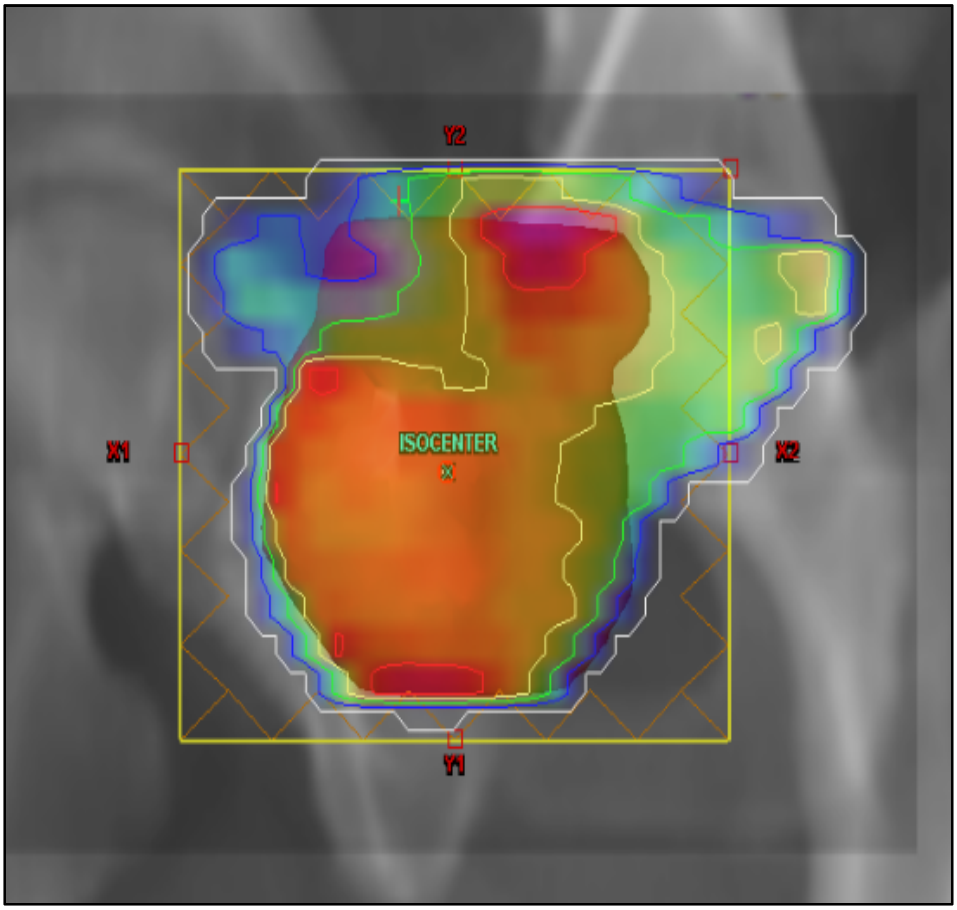

Figure 11: Image of the non-deformed match fluence super-imposed on query PTV

In figure 12, the deformed match fluence superimposed on the query PTV has the shape of the query PTV.

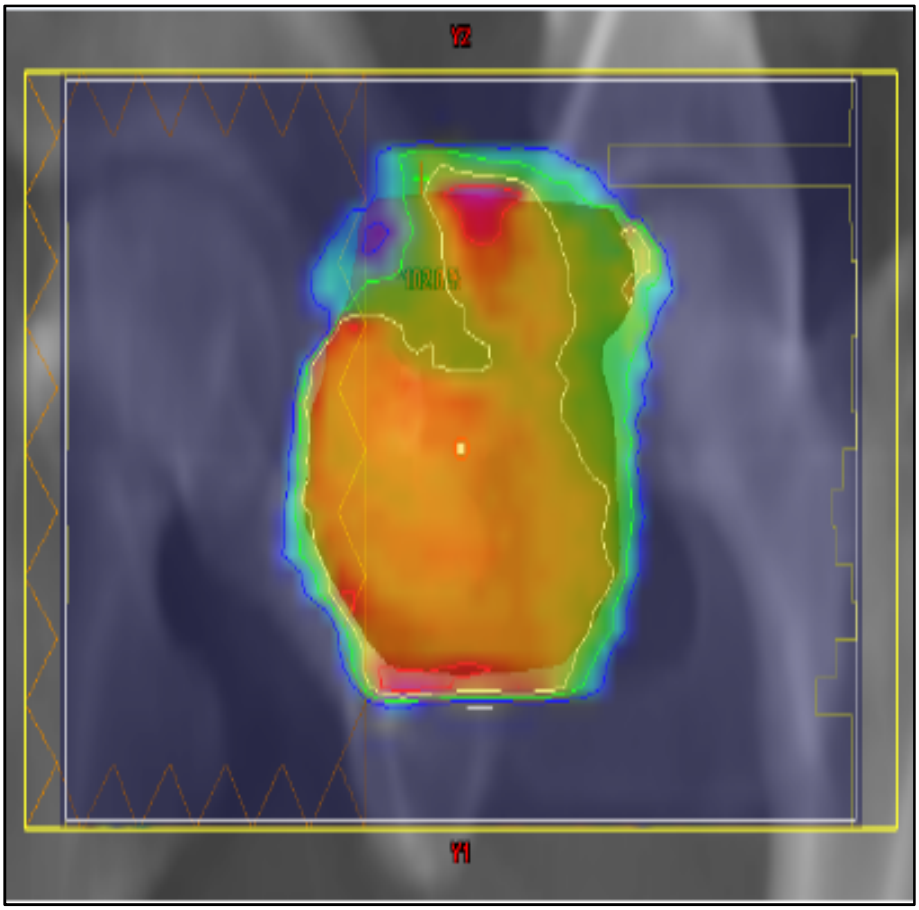

Figure 12: Image of the deformed match fluence superimposed on the query PTV

The deformed fluences for each of the seven angles are then imported into the Eclipse treatment planning system. While planning, the prescription dose for the query case will be the same as the match case. The prescription dose is the amount of radiation prescribed by the radiation oncologist which is determined by criteria such as the treatment site. The plan normalization mode for the query case will also be the same as the match case. These tricks are used as the fluences being imported into the eclipse treatment planning station for the query patient have dose patterns based on the

prescription dose and the plan normalization mode of the match case. By keeping these terms the same, more accurate results from the planning process would be obtained.

After the 3D dose has been calculated to create the pre-optimized plan, the prescribed dose and the plan normalization are switched such that 100% of the prescribed dose covers 95% of the PTV for the purposes of comparison. The dose patterns of the deformed match fluence were designed for the anatomy of the match case such that the dose to the OARs is minimized while the PTV dose is maximized. To make the dose patterns achieve these goals in the query case, the fluence needs to be further optimized. For the optimization of the query plan, the constraints were directly imported from the match case and 50-100 iterations (without manual intervention) of the Eclipse optimization engine were performed. After optimization, the dose is calculated again to produce the post-optimized plan.

2.4 Plan Quality Evaluation

After the planning process, the dose volume histograms (DVH) are generated for the original, pre-optimized and post-optimized query plans and exported from Eclipse. The DVH graphically summarizes the simulated radiation distribution within the PTV, bladder and rectum of a patient which would result from the proposed radiation treatment plan. However, due of the loss of spatial information in these volumes, DVHs are not the sole criteria for plan quality evaluation.

The homogeneity index (HI)[28] is one other way to quantify how homogenous the dose is across the PTV. Equation 3 below demonstrates how the HI is calculated.

$$HI = \frac{D_2 - D_{98}}{D_p} * 100$$

where D_2 is the dose that the highest 2% of the volume receives

D_{98} is the dose that the highest 98% of the volume receives

D_p is the prescription dose

Another metric used to express the homogeneity of the dose distribution in the PTV is the sigma index (S-Index). The S-Index is defined as the standard deviation of the normalized differential dose volume histogram curve (DVH)[28] and is calculated as shown in equation 4 below.

$$S - Index = \sqrt{\sum (D_i - D_{mean})^2 * \frac{v_i}{V}}$$

where D_i is the dose that is delivered to volume, v_i

V is the total volume of the target

$$D_{mean} = \sum_i D_i * \frac{v_i}{V}$$

A small value for the HI and S-Index indicate that the dose to the organ, specifically the PTV, receives as homogenous dose.

The goal of any radiation treatment is to not only deliver the prescribed dose homogeneously across the PTV but also minimize the dose delivered to the OARs. At

the Duke University Radiation Oncology Department, the IMRT prostate constraints used are shown in Table 1 below. To quantitatively determine the success of reducing the dose to the OARs, the volumes receiving over 40Gy and 65Gy are incorporated in the analysis.

Table 1: Table showing the volume and dose constraints for the bladder, rectum and PTV

	Dose (Gy or %)	Volume (Absolute or %)
Bladder	75Gy	<10cc
Bladder	65Gy	25%
Bladder	40Gy	40%
Rectum	75Gy	<10cc
Rectum	65Gy	17%
Rectum	40	40%
PTV	102% of PD	0%
PTV	98% of PD	100%

The prescribed doses for prostate cancer cases range from 60Gy to 77Gy. In most courses of radiation, there is a primary and a boost plan which, when summed, gives the prescribed dose. In this study, only primary plans are being re-planned using the knowledge-based treatment planning methodology resulting in only a portion of the prescribed dose being delivered. This could result in misleading results since the

primary plan of one case could have a lower prescription dose due to an existing boost plan and thus may never deliver the dose constraints to the volumes of the OAR. By taking the ratio described in equation 6, all the plans will use a scaled dose constraint which is dependent on the prescribed dose.

$$Dose_{Constraint} = \frac{Prescribed\ Dose\ (cGy)}{7600\ cGy} * (4000cGy\ or\ 6500cGy)$$

Despite all efforts to eliminate the dose from the OARs, they do receive dose in order to effectively target the PTV. The dose the OAR receives is proportional to the probability of consequent complications. The Normal Tissue Complication Probability (NTCP), shown in equation 8, measures that likelihood of complications in the organ of interest given a specific delivered dose.

$$NTCP = \frac{1}{\sigma\sqrt{2\pi}} \int_{-\infty}^{D} e^{-\left(\frac{(x-TD_{50})^2}{2\sigma^2}\right)} dx$$

where $\sigma = mTD_{50}$

m is the slope of the complication probability vs. dose curve [29]

TD_{50} is the tolerance dose for 50% probability of injury

D is the uniform dose

One of the assumptions of the NTCP measure is that a uniform dose is being delivered to organ. However, the dose to the OARs is not uniform. Therefore, in order to

use the NTCP measure for the OARs, an equivalent uniform dose (EUD) is calculated as shown in equation 9.

$$EUD = \left(\frac{\sum_i V_i \, D_i^{1/n}}{\sum_i V_i} \right)^n$$

where V_i is the volume at dose D_i

n is the volume dependence of the complication probability [29]

The NTCP equation then becomes

$$NTCP = \frac{1}{\sigma\sqrt{2\pi}} \int_{-\infty}^{EUD} e^{-\left(\frac{(x-TD_{50})^2}{2\sigma^2}\right)} dx$$

The terms, listed in Equations 8 and 9, needed to generate the NTCP values for the bladder and rectum are shown in Table 2 below.

Table 2: Table of showing the variables needed to calculate NTCP for the bladder and rectum

Organs	M	n	TD_{50}
Bladder	0.11	0.5	80Gy
Rectum	0.15	0.12	80Gy

The Wilcoxon signed rank test was used to determine the success of reducing the dose to the OARs. It is non-parametric test computed by summing the ranked differences of the deviation of each variable from a median above the hypothesized

value[30]. The DVH cut points, HI-Index, S-Index and NTCP are the metrics used to measure the dosimetric quality of the treatment plans. The Wilcoxon signed rank test is then used to determine if the plans generated by the knowledge-based approach are significantly better or worse than the original plans by comparing the medians of the two distributions (original plans and the knowledge-based generated plans) when using the DVH cut points and NTCP metrics.

The changes made in the methodology of the knowledge-based approach employed by our previous group[22] were done to effectively determine the best match case for each query case and to reduce the dependence of the planner's subjectivity on the treatment planning process.

3. Planning Target Volume (PTV) Evaluation

Separate evaluations of the PTV and OARs are used in order to investigate the dosimetric quality of the treatment plans. To assess the plan quality of the prior clinically approved treatment plans and the knowledge-based generated treatment plans, the differential and cumulative DVHs are used.

3.1 Dose Volume Histograms (DVH)

DVHs graphically summarize the simulated radiation distribution within the PTV, bladder and rectum of a patient which would result from the proposed radiation treatment plan[31]. The DVH curves are graphed such that the y-axis represents the percent volume and the x-axis represents the percent dose. The area under the PTV curve should be maximized such that 100% of the prescribed dose is delivered to 100% of the target volume. A portion of the target volume that receives a dose greater than 100% of the prescribed dose is considered to be a hotspot and a volume that receives a dose less than 100% of the prescribed dose is considered to be a cold spot. The area under the OARs should be minimized to indicate that the dose to the bladder and rectum is minimal.

Below are nine examples of DVHs (Figures 13 - 21) which are representative of the PTV trends observed from the 101 planned cases. Note that the original plan is the plan generated by manually adjusting the plan optimization objectives; the pre-

optimized plans were generated with the deformed fluences only and the post-optimized plans were generated as a result of the optimization of the deformed fluences.

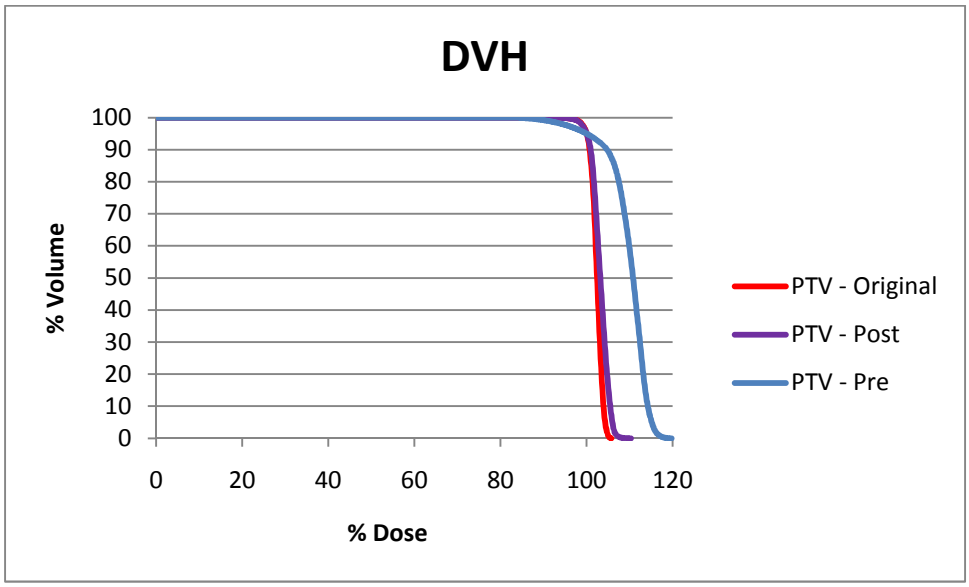

Figure 13: PTV DVH for query case 12 and match case 3 showing that the Post-optimized plan is comparable to the Original plan (Trend 1)

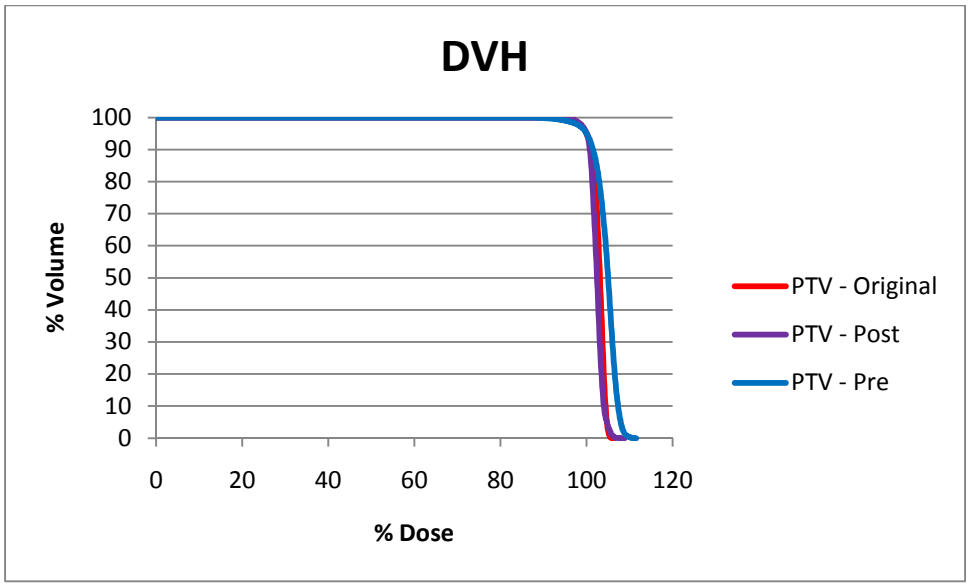

Figure 14: PTV DVH for query case 48 and match case 44 showing that the Post-optimized plan is comparable to the Original plan (Trend 1)

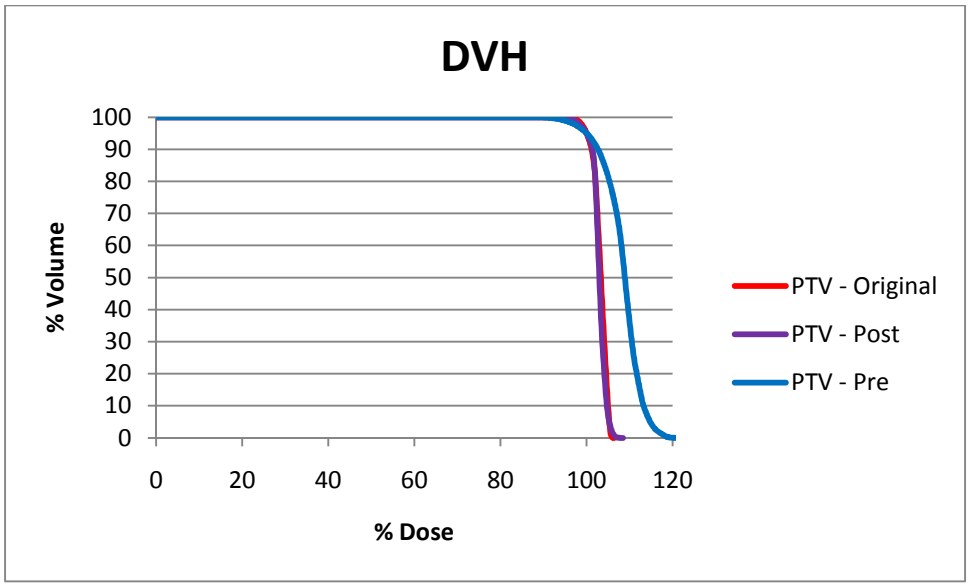

Figure 15: PTV DVH for query case 130 and match case 99 showing that the Post-optimized plan is comparable to the Original plan (Trend 1)

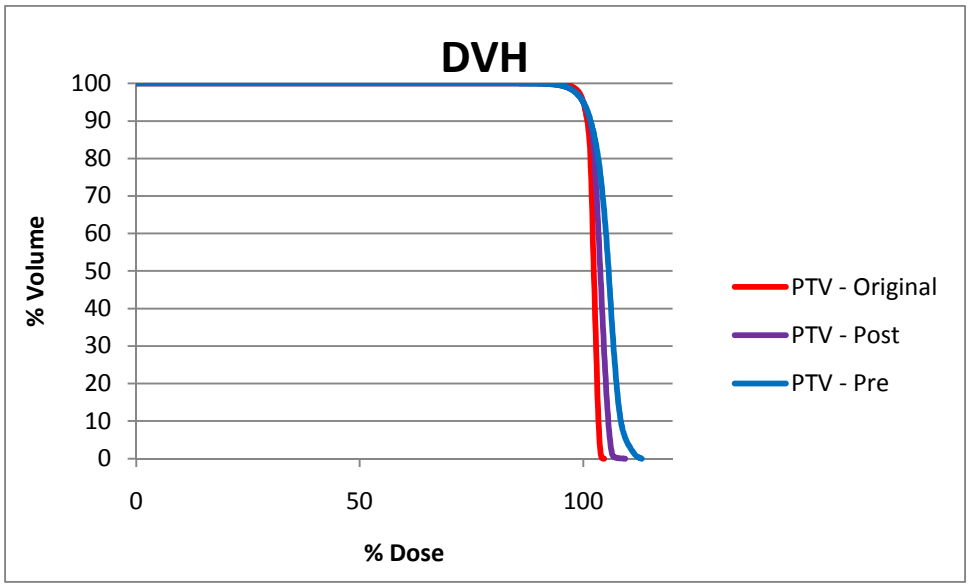

Figure 16: PTV DVH of query case 66 and match case 45 showing that the post-optimized plan delivers a higher dose to the PTV than the original plan (Trend 2)

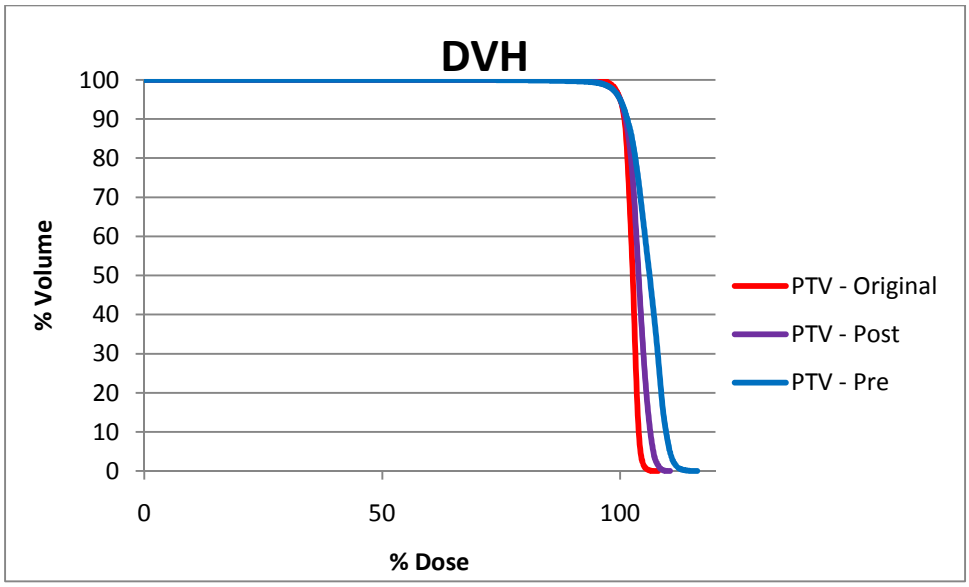

Figure 17: PTV DVH of query case 7 and match case 18 showing that the Post-optimized plan delivers a higher dose to the PTV than the Original plan (Trend 2)

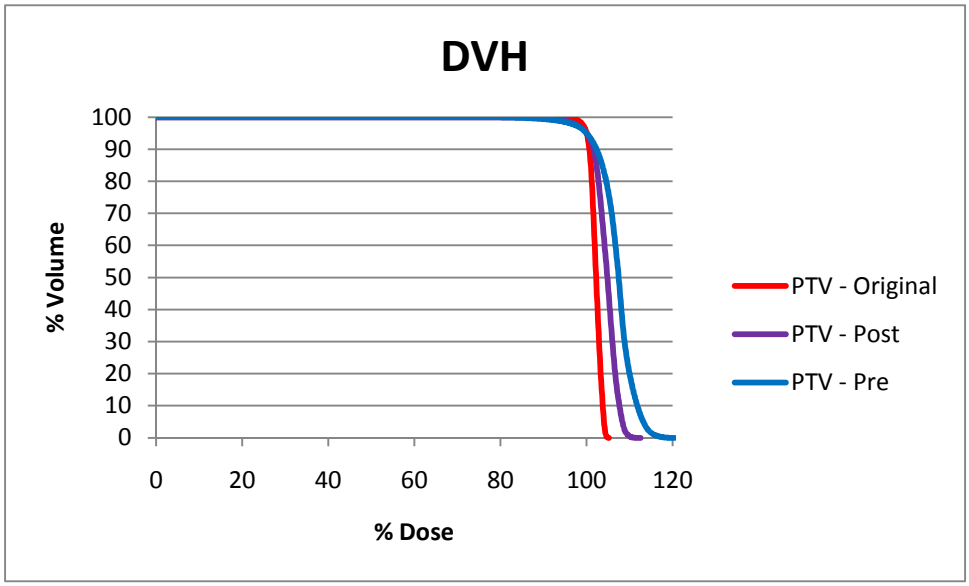

Figure 18: PTV DVH of query case 100 and match case 43 showing that the post-optimized plan delivers a higher dose to the PTV than the original plan (Trend 2)

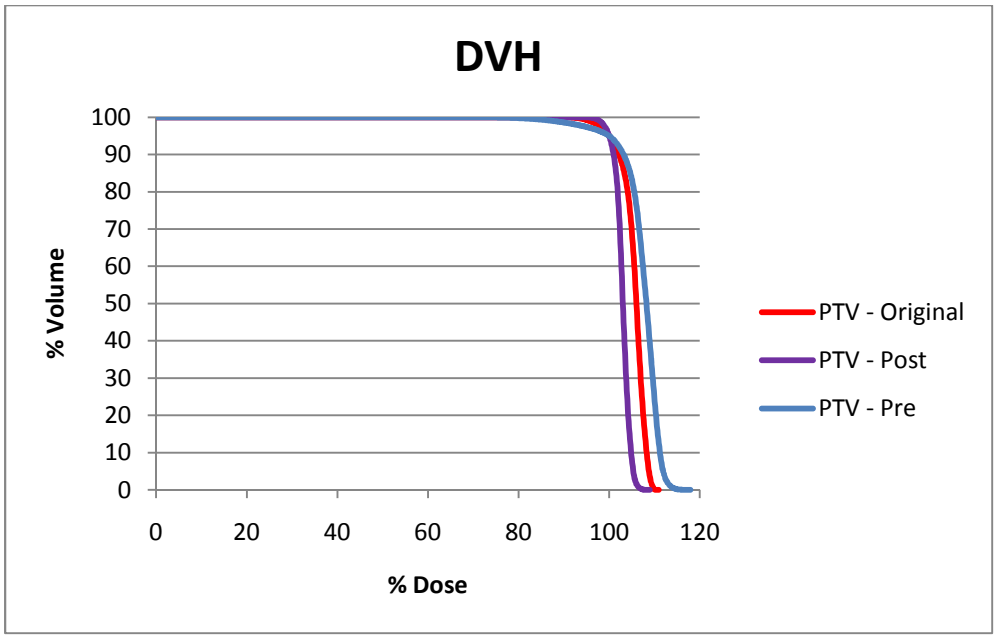

Figure 19: PTV DHV of query case 37 and match case 183 showing that the Post-optimized plan delivers a more optimal dose than the Original plan (Trend 3)

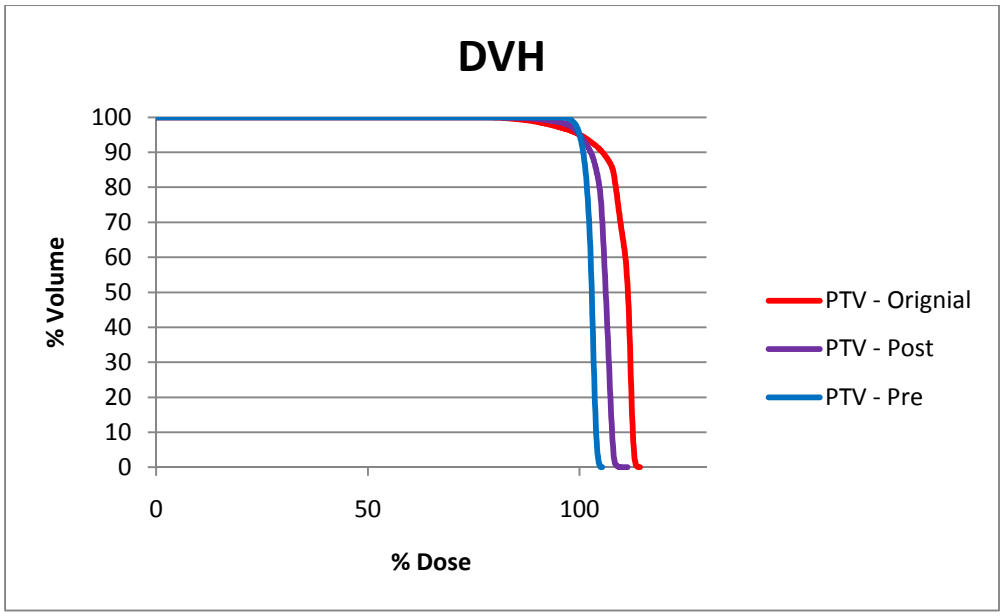

Figure 20: PTV DHV of query case 92 and match case 115 showing that the Post-optimized plan delivers a more optimal dose than the Original plan. (Trend 3) Note that the Pre-optimized plan delivers the most optimal dose to the PTV.

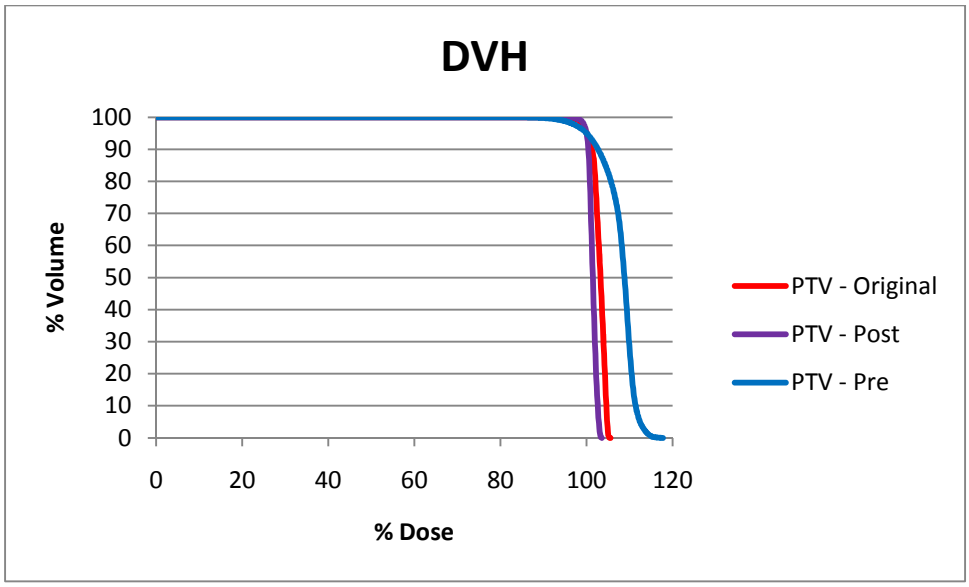

Figure 21: PTV DHV of query case 182 and match case 44 showing that the Post-optimized plan delivers a more optimal dose than the Original plan (Trend 3)

Figures 13 -21 show the three (3) dosimetric trends (trends 1, 2 and 3 respectively) of the PTV observed for the 101 planned cases: the original plan PTVs are comparable to the post-optimized PTVs (Figures 13-15), the post-optimized plan delivers a dose higher than the prescription dose to the PTV than the original plan (Figures 16-18) and the post-optimized plans deliver a more therapeutic dose to the PTV than the original plans (figures19-21). Trend 1 was observed for 66.3% the 101 planned cases; Trend 2 was observed for 28.7% of the planned cases and trend 3 was observed for 4.95% of the cases. For the pre-optimized plans, 85.1% of the cases delivered a dose higher than the prescription dose to the PTV than the original plan, 13.8% delivered a dose comparable to the original plan (Figure 14) and 1 case delivered a more therapeutic dose than the original plan (Figure 20).

One of the main goals of a treatment plan is to deliver the prescribed dose to the target tumor. A dose that is <95% of the prescribed dose is considered suboptimal. However, a dose that is >110% of the prescribed dose could result in undesired radiation toxicity. The trends shown in Figures 13, 15 - 19 indicate that the pre-optimized plans do not produce an optimal dose to the PTV as the dose is either suboptimal or may result in undesired radiation toxicity.

The post-optimized plans are comparable to the original plans, deliver doses to the PTV that are higher than the original plans or deliver a more optimal dose to the PTV than the original plans. Trend 1 was observed for 66.3% of the planned cases which indicates that 67 out of 101 times, the pre-optimized plans are equivalent in delivering a therapeutic dose to the PTV as the originally planned course of treatment. In other words, the knowledge-based approach to treatment planning is as effective as the original plans in delivering the prescribed dose to the PTV.

3.2 Planning Target Volume (PTV) Homogeneity

The PTV is the target of the course of radiation being delivered to the patient. A homogenous dose is desirable in the PTV since lower doses are suboptimal and high doses could result in radiation toxicity e.g. necrosis. The homogenous dose delivered to the patient should ideally be the dose prescribed by the radiation oncologist. To quantitatively determine the homogeneity of the dose being delivered to the PTV, the

average HI-Index and S-Index of the 101 cases, as indicated by Equations 3 and 4, are summarized in Table 3 below.

Table 3: Average S-Index and HI-Index values for the pre-optimized, post-optimized and originally planned cases

	Pre-Optimized Plan	Post-Optimized Plan	Original Plan
S-Index	4.65 ± 2.29	2.11 ± 0.87	1.52 ± 0.48
HI-Index	20.1 ± 9.87	8.97 ± 4.07	6.52 ± 2.12
Mean % Dose	108.9%	103.6%	102.6%

Table 3 shows that the homogeneity of the dose being delivered to the PTV is greatest in the original plans as indicated by both the S-Index and HI-Index. On average, the dose to the PTV for the original planned cases were 27% more homogenous than the post-optimized cases and 67% more homogeneous than the pre-optimized cases (trend 4) according to the S-Index and HI-Index. The trend observed is expected as the cases being compared are all from Duke University's Radiation Oncology department. Since the test cases and the knowledge base are drawn from the same pool of plans, on average, it is not possible for the new plans to improve upon the original plans. In other words, the cases generated from the knowledge-based model will necessarily be of equal or lesser dosimetric quality than the originally planned cases.

To graphically understand trend 4 indicated by Table 3, the cumulative and differential DVH are used. The HI-Index is a basic measure of the deviation of the PTV

slope in the cumulative DVH from the vertical line at prescription dose (100% dose line). From Figures 16 - 18, the pre-optimized PTV curve deviates more from the vertical line than the post-optimized PTV curve and the originally planned case deviates the least indicating that the originally planned cases delivers the most homogenous dose to the PTV and the pre-optimized delivers the least homogenous dose to the PTV. This is observed for greater than 99% of the cases planned.

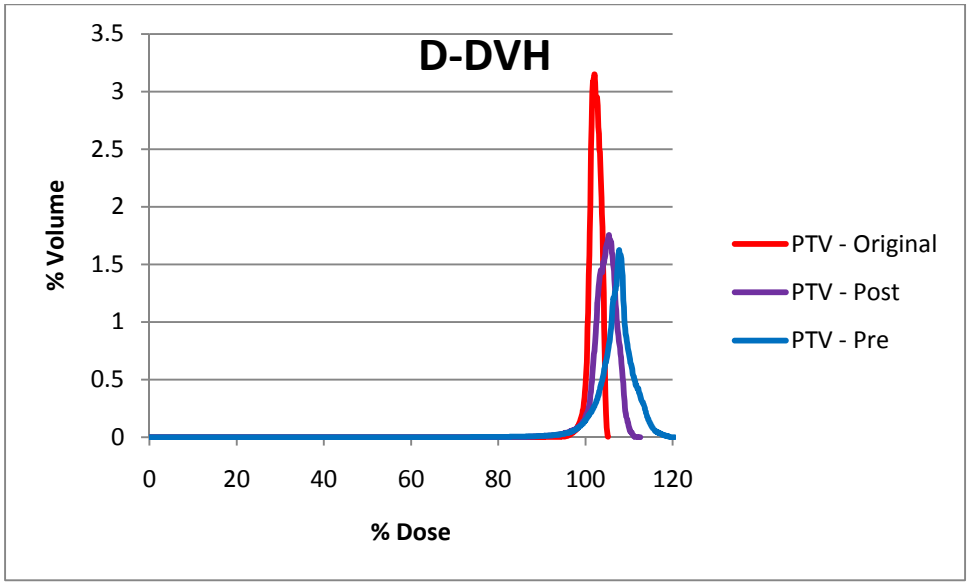

Figure 22: Differential DVH of the PTV for query case 100 and match case 43 showing that the deviation from the mean is greatest for the Pre-optimized plans and smallest for the Original plan. This figure also shows that the mean %dose to the PTV is greatest in the pre-optimized plans and the least in the original plans

The S-Index is the deviation from the mean dose of the differential DVH. With an increase in the deviation from the mean dose, there is a corresponding decrease in the

homogeneity of the dose being delivered to the PTV. Figure 22 shows that the largest deviation occurs with the pre-optimized plans whereas the least deviation occurs in the originally planned cases.

The mean % dose in Table 3, calculated as shown in Equation 4, show that the mean dose to the PTV is approximately 109% of the prescribed dose for the pre-optimized plans, 104% for the pre-optimized plans and 103% for the original plans. An example of this is shown in Figure 22. The dose to the target volume should ideally be 100% of the prescribed dose which is best achieved by the original plans. However, an average dose that is equivalent to the prescribed dose is not the only factor that determines the efficacy of the treatment plan. The homogeneity of the dose across the PTV is equally as important in delivering an effective course of radiation.

4. Organs-at-risk (OAR) Evaluation

Dose to the OARs should be limited in order to decrease the probability of complications in those organs. For IMRT of prostate cancer, these dose limiting organs are represented by the bladder and the rectum. The dose constraints, Wilcoxon signed rank test and the normal tissue complication probability (NTCP) values are used to compare the dosimetric quality of the bladder and rectum of the previously planned cases and the treatment plans generated by the knowledge-based approach.

4.1 Dose Volume Histograms

The knowledge-based pre-optimized plans delivered the highest doses to the OARs in comparison to the knowledge-based post-optimized plans and the original plans. As a result, this paper will only compare the dose delivered to the OARS by the knowledge-based post optimized plans and the original plans.

Figures 23 – 29 are representative of the three OAR trends observed in the 101 planned cases. Note that the original plan is the plan generated by manually adjusting the plan optimization objectives and the post-optimized plans were generated as a result of the optimization of the deformed fluences.

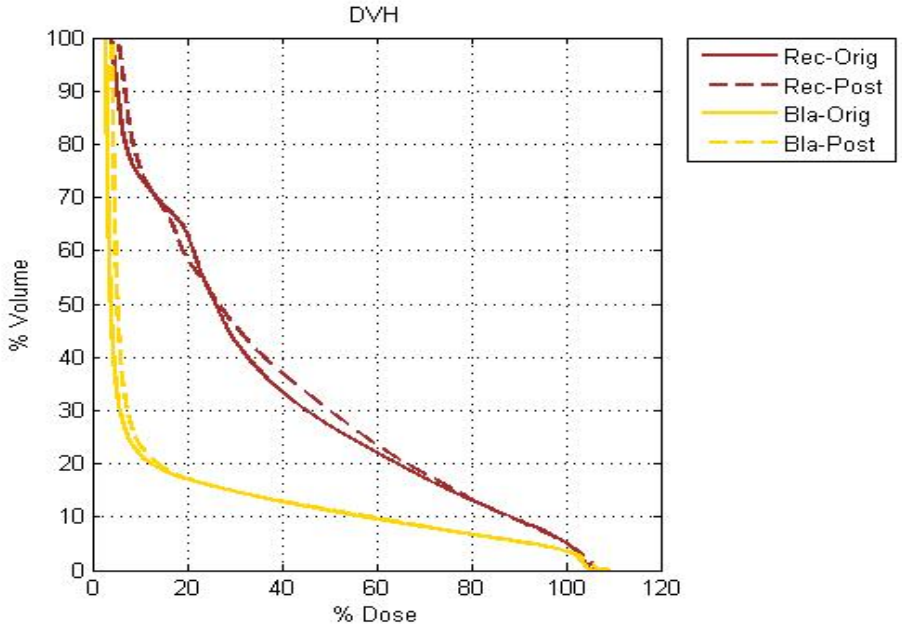

Figure 23: OAR DVH of query case 23 and match case 182 showing that the Post-optimized plan is comparable to the Original plan (Trend 1)

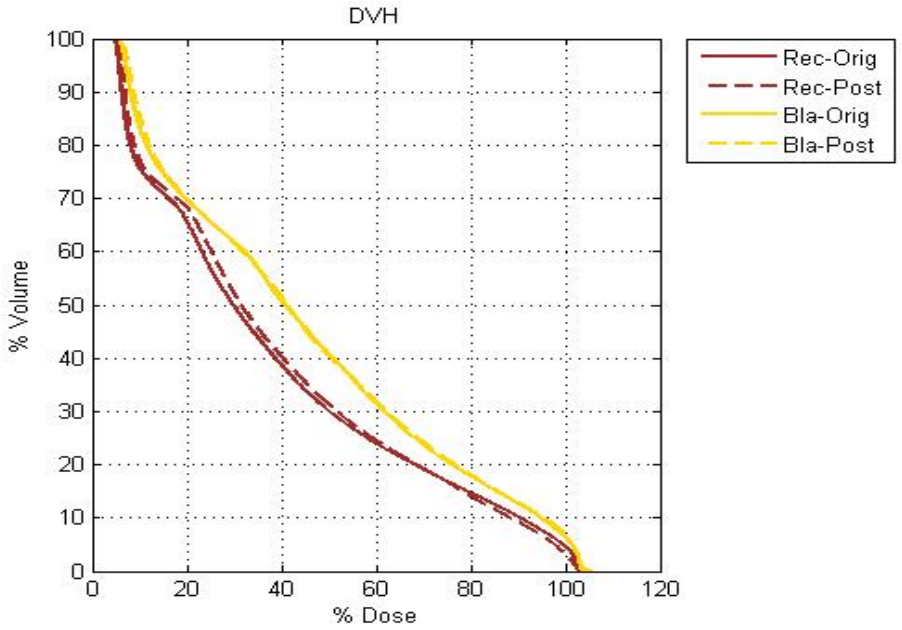

Figure 24: OAR DVH of query case 38 and match case 214 showing that the Post-optimized plan is comparable to the Original plan (Trend 1)

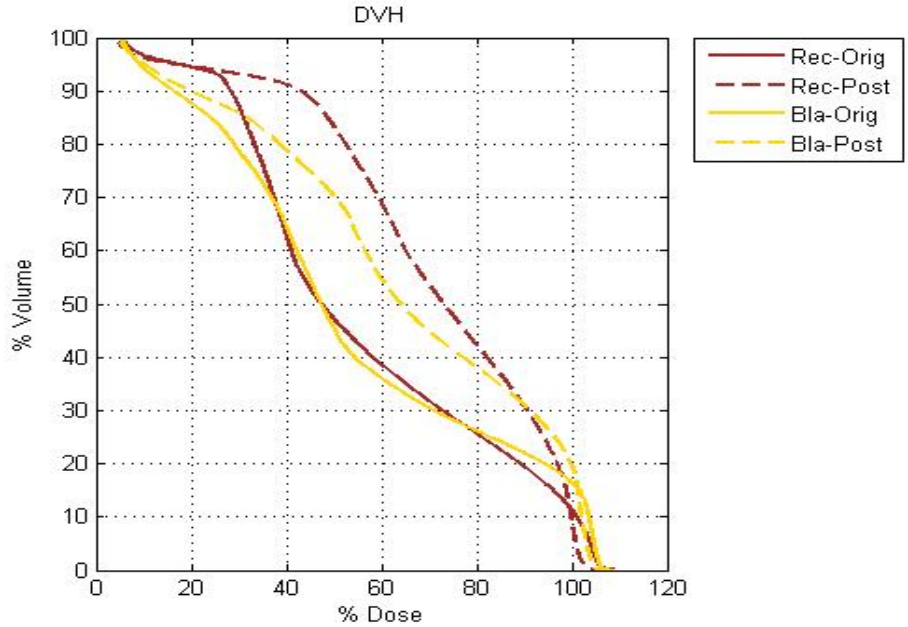

Figure 25: OAR DVH of query case 35 and match case 161 showing that the post-optimized plan delivers a higher dose to the OARs than the original plan (Trend 2)

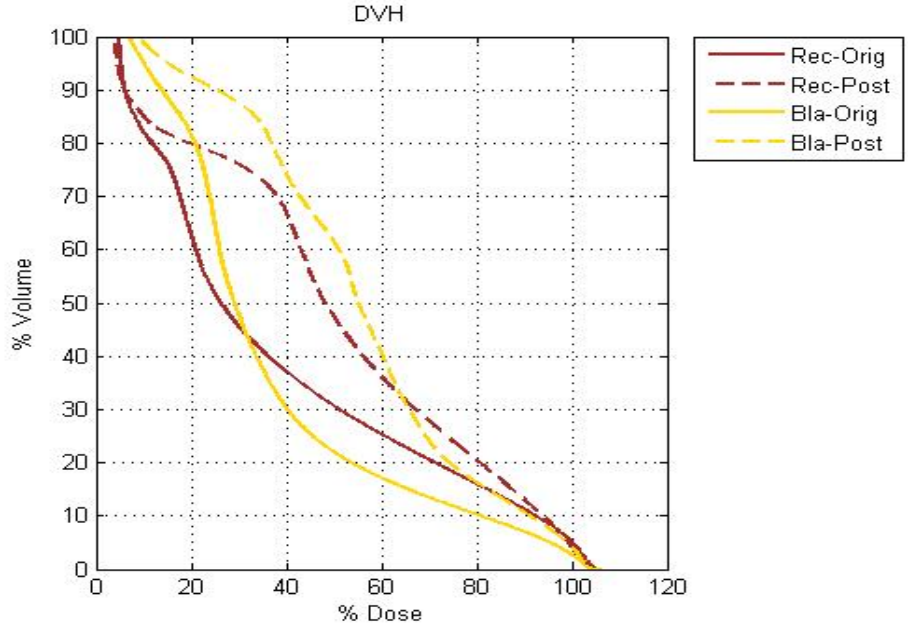

Figure 26: OAR DVH of query case 53 and match case 173 showing that the post-optimized plan delivers a higher dose to the OARs than the original plan (Trend 2)

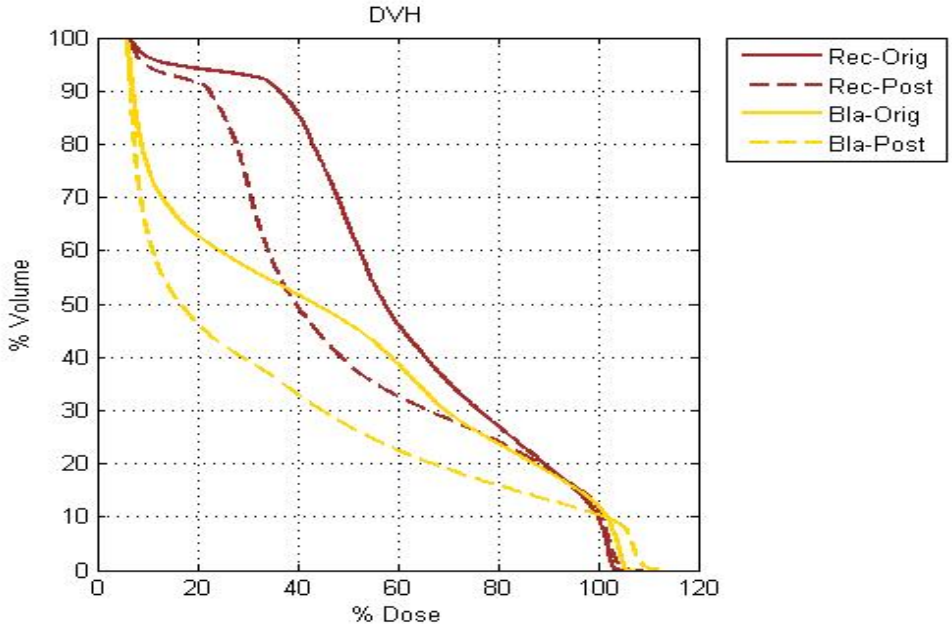

Figure 27: OAR DVH of query case 9 and match case 199 showing that the post-optimized plan delivers a lower dose to the OARs than the original plan (Trend 3)

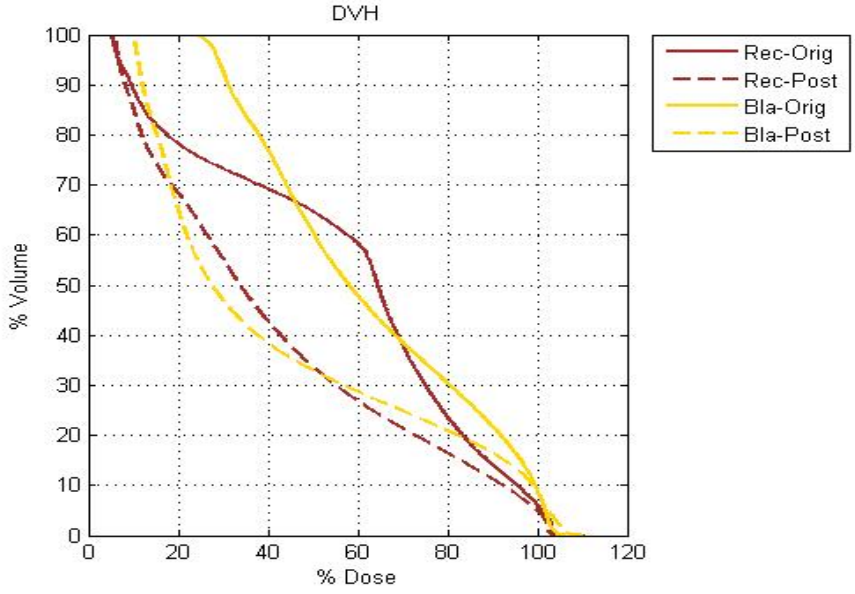

Figure 28: OAR DVH of query case 180 and match case 207 showing that the post-optimized plan delivers a lower dose to the OARs than the original plan (Trend 3)

The three trends observed are described as follows; Trend 1 describes the dose delivered to the specific organ at risk by the post-optimized plan as being comparable to the original plan (Figures 23 & 24); Trend 2 describes the dose delivered by the post-optimized plan is greater than the original plan (Figure 25 &26) and Trend 3 describes the dose delivered to the OAR by the post-optimized plan is less than what is delivered by the original plan (Figures 27 &28). Trends 1, 2 and 3 are observed in 42%, 15% and 43% of the cases for the bladder and 37%, 21% and 43% for the rectum respectively. This shows that for 85% and 77%of the cases, the dose delivered to the bladder and rectum respectively is either comparable or lower with the post-optimized plans than the original plans.

4.2 Dose Constraints

The scaled dose constraints for the 40Gy and 65Gy cut points (see Equation 6) are displayed in Figures 29 -32 for the bladder and the rectum for the post-optimized and original plans. The trendlines used Figures 29 – 32 are generated such that the intercept passes through zero (0).

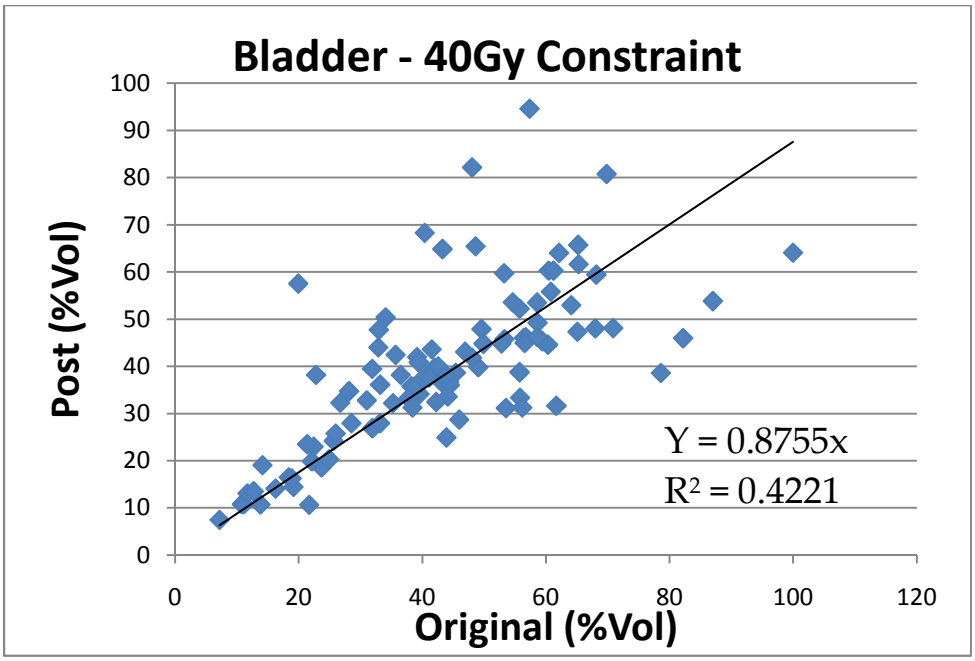

Figure 29: Graph showing the % volume for the post-optimized plan versus the original plan for the bladder at the scaled 40Gy constraint

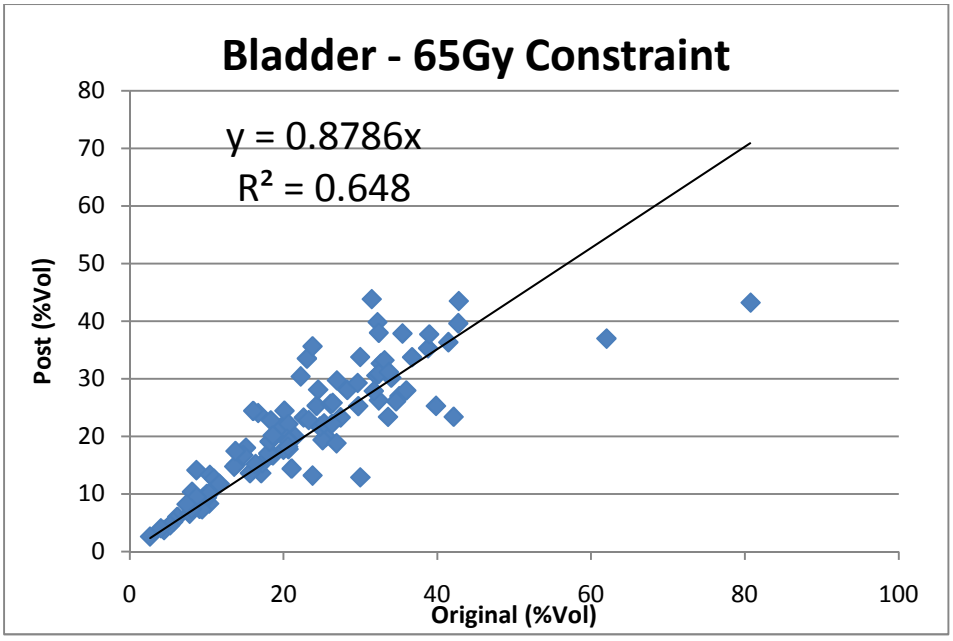

Figure 30: Graph showing the % volume for the post-optimized plan versus the original plan for the bladder at the scaled 65Gy constraint

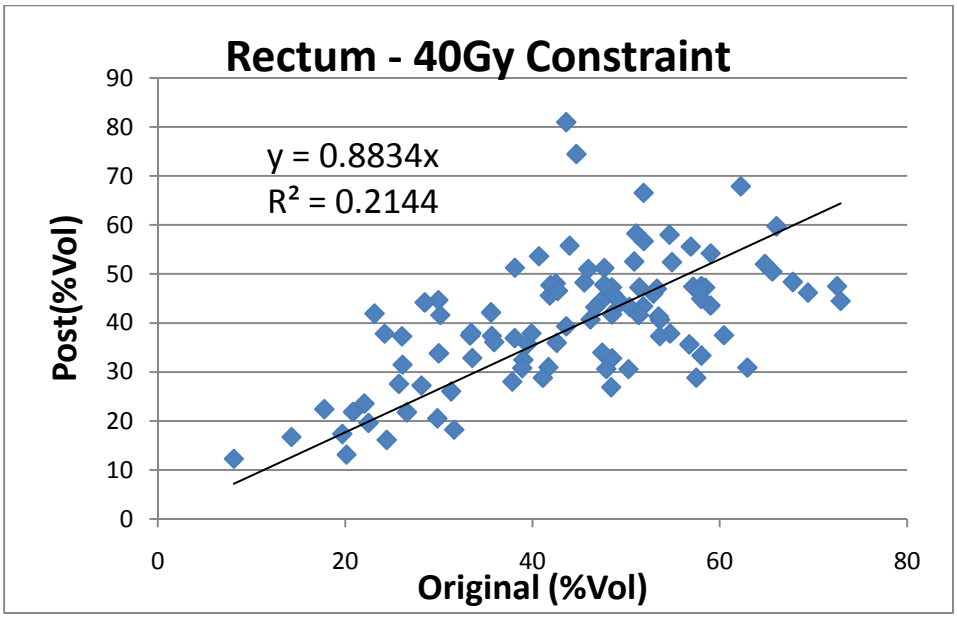

Figure 31: Graph showing the % volume for the post-optimized plan versus the original plan for the rectum at the scaled 40Gy constraint

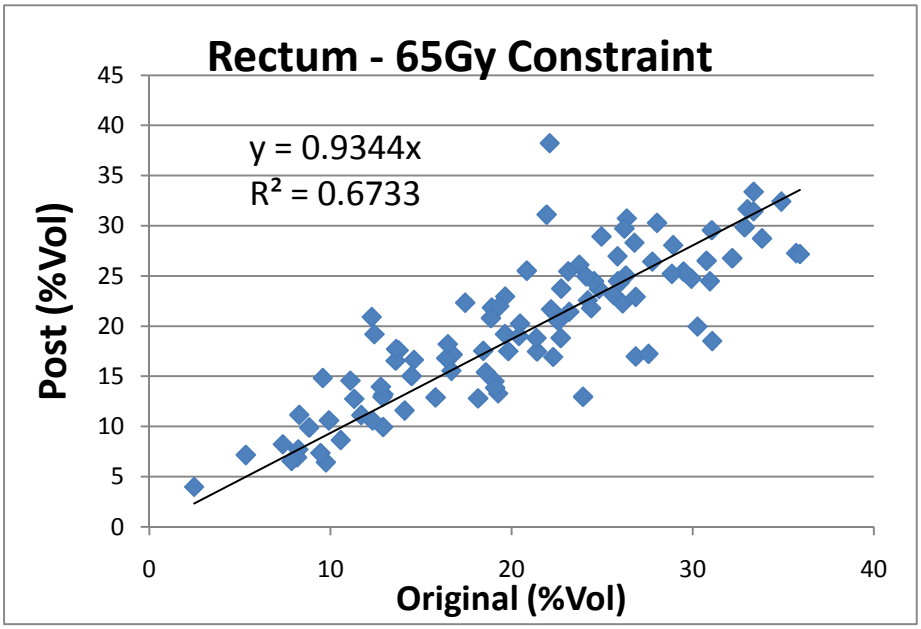

Figure 32: Graph showing the % volume for the post-optimized plan versus the original plan for the rectum at the scaled 65Gy constraint

Figures 29 – 32 show that the slope of the graphs are consistently just below 1 (range from 0.87 to 0.93), which indicates that the post-optimized plans delivers the specified dose to a smaller volume than the original plans. In other words, the new knowledge-based plans produce DVH curves that, on average, are comparable to the original plans'.

Another means of determining the dosimetric quality of the treatment plans is to explore the difference in the % volume for the scaled 40Gy and 65Gy dose constraints between the post-optimized and original plans. (See Table 4 below)

Table 4: Average difference in % Volume and the Wilcoxon signed rank test p values for the post-optimized plans and the original plans

Organs	40Gy Cut Point		65Gy Cut Point	
	Average % Volume	P value	Average % Volume	P value
Bladder	-3.6 ± 13.3	<0.001	-1.5 ± 6.6	0.018
Rectum	-3.7 ± 11.9	0.0013	-0.8 ± 4.3	0.025

From Table 4 above, the negative values indicate that the average % volume receiving a specified dose is lower for the post-optimized plan than the original plan. This trend is observed for both dose constraints and both OAR structures. However, the standard deviations are so large that the small differences are not clinically significant. This indicates that the post-optimized plans are comparable to the original plans

signifying that the knowledge-based approach delivers a dose to the bladder and rectum equal to the traditional approach to IMRT treatment planning.

The Wilcoxon signed rank test compares the median of one distribution to another and determines the similarity between the two sets of data. The results of comparing the post-optimized plan distributions for the bladder and rectum with the original plans are tabulated as shown in Table 4. For both cutpoints of both structures (rectum and bladder), all of the differences were statistically significant ($p<0.05$) suggesting that the knowledge-based approach provides better dose savings to the OARs. As previously indicated, the actual differences are very small and not likely to be clinically significant. The statistically significant differences are likely due to the high degree of correlation between the DVH curves.

4.3 Normal Tissue Complication Probability (NTCP)

Though the aim of a course of radiation is to minimize the dose to the OARs, some dose is delivered which may cause complications in the bladder and rectum. The NTCP value gives the probability of complications due to a uniform dose delivered to the OARs. The NTCP values for the rectum and bladder are shown in Table 5.

Table 5: Average NTCP and the Wilcoxon signed rank test p values for the post-optimized and original treatment plans

Organs	Post-Optimized	Original	P values
Bladder	$(0.63 \pm 2.9) * 10^{-4}$	$(3.08 \pm 21.0) * 10^{-4}$	<0.001
Rectum	0.015 ± 0.015	0.014 ± 0.014	0.47

The post-optimized plans are 82.8% less likely to cause complications in the bladder than the original plans. For the rectum, the probability of complication in the original plans and the post-optimized plans are nearly identical. This is also indicated by the p-value ($p>0.05$) where the medians for the two distributions are not statistically different from each. For the bladder, however, the NTCP values are statistically significant as indicated by the p-value <0.001. This shows that median of the two distributions (original bladder and post-optimized bladder) are significantly different from each other. However, because the probability of complications in the bladder is so small (~0), the significant difference between the two distributions is clinically insignificant. From a clinical point of view, the probability of complications with either treatment planning method is negligible. Overall, the probability of complications in the bladder and rectum due to the dose delivered by the post-optimized plans and the original plans are comparable.

5. Summary, Conclusions and Future Work

5.1 Summary of Findings

The aim of a course of radiation treatment is to maximize the dose and coverage to the target volume (PTV) and minimize the dose to surrounding organs-at-risk (bladder and rectum). Manual IMRT treatment planning is a time consuming technique used to achieve this goal. The knowledge-based approach to IMRT treatment planning is the solution offered to reduce the treatment planning time and generate high quality treatment plans by minimizing the dose to the OARs and maximizing the therapeutic dose to the PTV.

The knowledge-based methodology begins with the development of a database of prior clinically approved IMRT treatment plans obtained from the Duke Clinic. A case-similarity algorithm incorporating mutual information (MI) is used to compare the anatomy of the cases within in the database. To validate the performance of the proposed system, a query case is selected from the database and acts as a new patient that needs a treatment plan. Using the Eclipse treatment planning system, the match case with the highest MI value among the remaining cases is used to generate a treatment plan for the query case. The dosimetric quality of the treatment plans produced by the knowledge-based approach is compared to the plans created manually. The PTV and OARs were evaluated separately in Chapters 3 and 4, respectively. The figure of merit used included dose volume histograms, homogeneity indices, dose-

volume criteria and normal tissue complication probabilities (NTCP) from the treatment plans.

In spite of the matching and subsequent registration procedure, the pre-optimized plans do not deliver sufficient dose to satisfy target homogeneity or sufficiently avoid normal organs. After automated optimization with the clinical treatment planning system, however, the post-optimized plans deliver a dose to the PTV that is comparable to the original plans, deliver a more therapeutic dose to the PTV than the original plans or deliver a more suboptimal dose to the PTV than the original plans. On average, the dose to the PTV for the original planned cases were 27% more homogenous than the knowledge-based post-optimized cases and 67% more homogeneous than the knowledge-based pre-optimized cases according to the S-Index and HI-Index.

For the bladder and rectum, the average % volume that receives the scaled 40Gy and the scaled 65Gy dose in the post-optimized plans is statistically significantly less than the original plans, but these differences were very small and not likely to be clinically significant. From Table 5, the NTCP values indicate that the post-optimized plans are 82.8% less probable to cause complications in the bladder than the original plans. For the rectum, the post-optimized plans and the original plans are comparable. Overall, these encouraging results suggest that post-optimized plans and the original plans are comparable.

5.2 Future Work

The knowledge-based methodology has demonstrated the ability to produce treatment plans of comparable dosimetric quality in less time than traditional IMRT treatment planning. However, there are extensions to this work that could increase the efficacy of the treatment plans generated.

Mutual Information (MI) is the key to the case-similarity algorithm employed by the knowledge-based methodology. Currently, mutual information is used to compare masks that consist of the PTV, bladder, rectum, right and left femoral heads. In some cases, the contours of the femoral heads include the shaft as well as the femoral head. In these cases, the MI value may artificially decrease when comparing cases with the femoral shafts and cases with only the femoral heads. These inconsistencies in femoral head contouring may negatively impact the similarity matching process. A solution to this issue would be comparing masks that consist of only the most important structures, namely the bladder, rectum and PTV.

Once a match has been established by the case-similarity algorithm, the fluences are deformed in order to adapt the match case's treatment plan to the query case's anatomy. The 2D deformations of the fluences are done at each of the treatment angles. Deforming the 3D fluence map instead of the 2D projections of the fluence map, may potentially improve the dosimetric quality of the knowledge-based generated treatment plans.

To demonstrate the feasibility for this new treatment planning approach, this study focused on IMRT of prostate cancer due to the high prevalence as well as the relatively simple anatomical constraints. The knowledge-based approach to IMRT treatment planning has the potential to be extended to other treatment sites that are more difficult and time-consuming to plan such as head & neck cases.

5.3 Conclusions

The manual IMRT treatment planning process is solely dependent on the expertise of the planner and requires a substantial amount of time to produce a treatment plan of clinical quality. The knowledge-based treatment plans are created by adapting the anatomy of a previously planned patient to that of a new patient and requires no manual intervention. The post-optimized treatment plans produced by the knowledge-based approach have demonstrated dosimetric quality equivalent to the treatment plans created by the human planner and in a fraction of the time.

This work has the potential to automatically provide high quality treatment plans while dramatically reducing treatment planning time. The main contribution of this study was to demonstrate feasibility for the new approach using 101 cases from this institution. Given the large size of this data set, the results are likely to be robust in representing treatment planning efficacy over a diverse range of patient anatomy.

Appendix A

Parameter File for B-spline Registration

```
// C-style comments: //
// The internal pixel type, used for internal computations
// Leave to float in general.
// NB: this is not the type of the input images! The pixel
// type of the input images is automatically read from the
// images themselves.
// This setting can be changed to "short" to save some memory
// in case of very large 3D images.
(FixedInternalImagePixelType "float")
(MovingInternalImagePixelType "float")
// The dimensions of the fixed and moving image
// NB: This has to be specified by the user. The dimension of
// the images is currently NOT read from the images.
// Also note that some other settings may have to specified
// for each dimension separately.
(FixedImageDimension 2)
(MovingImageDimension 2)
// Specify whether you want to take into account the so-called
// direction cosines of the images. Recommended: true.
// In some cases, the direction cosines of the image are corrupt,
// due to image format conversions for example. In that case, you
// may want to set this option to "false".
(UseDirectionCosines "true")

// *************** Main Components ************************
// The following components should usually be left as they are:
(Registration "MultiResolutionRegistration")
(Interpolator "BSplineInterpolatorFloat")
(ResampleInterpolator "FinalBSplineInterpolatorFloat")
(Resampler "DefaultResampler")
// These may be changed to Fixed/MovingSmoothingImagePyramid.
// See the manual.
(FixedImagePyramid "FixedRecursiveImagePyramid")
(MovingImagePyramid "MovingRecursiveImagePyramid")
// The following components are most important:
// The optimizer AdaptiveStochasticGradientDescent (ASGD) works
```

```
// quite ok in general. The Transform and Metric are important
// and need to be chosen careful for each application. See manual.
(Optimizer "AdaptiveStochasticGradientDescent")
(Transform "BSplineTransform")
(Metric "AdvancedMattesMutualInformation")

// **************** Transformation ************************
// The control point spacing of the bspline transformation in
// the finest resolution level. Can be specified for each
// dimension differently. Unit: mm.
// The lower this value, the more flexible the deformation.
// Low values may improve the accuracy, but may also cause
// unrealistic deformations. This is a very important setting!
// We recommend tuning it for every specific application. It is
// difficult to come up with a good 'default' value.
(FinalGridSpacingInPhysicalUnits 9)
// Alternatively, the grid spacing can be specified in voxel units.
// To do that, uncomment the following line and comment/remove
// the FinalGridSpacingInPhysicalUnits definition.
//(FinalGridSpacingInVoxels 16)
// By default the grid spacing is halved after every resolution,
// such that the final grid spacing is obtained in the last
// resolution level. You can also specify your own schedule,
// if you uncomment the following line:
//(GridSpacingSchedule 4.0 4.0 2.0 1.0)
// This setting can also be supplied per dimension.
// Whether transforms are combined by composition or by addition.
// In generally, Compose is the best option in most cases.
// It does not influence the results very much.
(HowToCombineTransforms "Compose")

// ****************** Similarity measure ********************
// Number of grey level bins in each resolution level,
// for the mutual information. 16 or 32 usually works fine.
// You could also employ a hierarchical strategy:
//(NumberOfHistogramBins 16 32 64)
(NumberOfHistogramBins 32)
// If you use a mask, this option is important.
// If the mask serves as region of interest, set it to false.
// If the mask indicates which pixels are valid, then set it to true.
```

```
// If you do not use a mask, the option doesn't matter.
(ErodeMask "false")

// ****************** Multiresolution ********************
// The number of resolutions. 1 Is only enough if the expected
// deformations are small. 3 or 4 mostly works fine. For large
// images and large deformations, 5 or 6 may even be useful.
(NumberOfResolutions 4)
// The downsampling/blurring factors for the image pyramids.
// By default, the images are downsampled by a factor of 2
// compared to the next resolution.
// So, in 2D, with 4 resolutions, the following schedule is used:
//(ImagePyramidSchedule 8 8  4 4  2 2  1 1 )
// And in 3D:
//(ImagePyramidSchedule 8 8 8  4 4 4  2 2 2  1 1 1 )
// You can specify any schedule, for example:
//(ImagePyramidSchedule 4 4  4 3  2 1  1 1 )
// Make sure that the number of elements equals the number
// of resolutions times the image dimension.

// ****************** Optimizer **************************
// Maximum number of iterations in each resolution level:
// 200-2000 works usually fine for nonrigid registration.
// The more, the better, but the longer computation time.
// This is an important parameter!
(MaximumNumberOfIterations 500)
// The step size of the optimizer, in mm. By default the voxel size is used.
// which usually works well. In case of unusual high-resolution images
// (eg histology) it is necessary to increase this value a bit, to the size
// of the "smallest visible structure" in the image:
//(MaximumStepLength 1.0)

// *************** Image sampling ********************
// Number of spatial samples used to compute the mutual
// information (and its derivative) in each iteration.
// With an AdaptiveStochasticGradientDescent optimizer,
// in combination with the two options below, around 2000
// samples may already suffice.
(NumberOfSpatialSamples 2048)
// Refresh these spatial samples in every iteration, and select
```

```
// them randomly. See the manual for information on other sampling
// strategies.
(NewSamplesEveryIteration "true")
(ImageSampler "Random")

// ************ Interpolation and Resampling ***************
// Order of B-Spline interpolation used during registration/optimisation.
// It may improve accuracy if you set this to 3. Never use 0.
// An order of 1 gives linear interpolation. This is in most
// applications a good choice.
(BSplineInterpolationOrder 1)
// Order of B-Spline interpolation used for applying the final
// deformation.
// 3 gives good accuracy; recommended in most cases.
// 1 gives worse accuracy (linear interpolation)
// 0 gives worst accuracy, but is appropriate for binary images
// (masks, segmentations); equivalent to nearest neighbor interpolation.
(FinalBSplineInterpolationOrder 3)
//Default pixel value for pixels that come from outside the picture:
(DefaultPixelValue 0)
// Choose whether to generate the deformed moving image.
// You can save some time by setting this to false, if you are
// not interested in the final deformed moving image, but only
// want to analyze the deformation field for example.
(WriteResultImage "true")
// The pixel type and format of the resulting deformed moving image
(ResultImagePixelType "short")
(ResultImageFormat "mhd")
```

References

1. Society, A.C. *Prostate Cancer*. 2011; Available from: http://www.cancer.org/acs/groups/cid/documents/webcontent/003134-pdf.pdf.

2. Society, A.C., *Prostate Cancer Statistics for 2012.* 2012.

3. Jolly, D., D. Alahakone, and J. Meyer, *A RapidArc planning strategy for prostate with simultaneous integrated boost.* J Appl Clin Med Phys, 2011. **12**(1): p. 3320.

4. Sze, H.C., et al., *RapidArc radiotherapy planning for prostate cancer: single-arc and double-arc techniques vs. intensity-modulated radiotherapy.* Med Dosim, 2012. **37**(1): p. 87-91.

5. Yoo, S., et al., *Radiotherapy treatment plans with RapidArc for prostate cancer involving seminal vesicles and lymph nodes.* Int J Radiat Oncol Biol Phys, 2010. **76**(3): p. 935-42.

6. Su, F.C., et al., *Dosimetric impacts of gantry angle misalignment on prostate cancer treatment using helical tomotherapy.* Technol Cancer Res Treat, 2008. **7**(4): p. 287-93.

7. Iori, M., et al., *Dose-volume and biological-model based comparison between helical tomotherapy and (inverse-planned) IMAT for prostate tumours.* Radiother Oncol, 2008. **88**(1): p. 34-45.

8. Grigorov, G., et al., *Optimization of helical tomotherapy treatment plans for prostate cancer.* Phys Med Biol, 2003. **48**(13): p. 1933-43.

9. Murthy, V., et al., *Does helical tomotherapy improve dose conformity and normal tissue sparing compared to conventional IMRT? A dosimetric comparison in high risk prostate cancer.* Technol Cancer Res Treat, 2011. **10**(2): p. 179-85.

10. Kairn, T., et al., *EBT2 radiochromic film for quality assurance of complex IMRT treatments of the prostate: micro-collimated IMRT, RapidArc, and TomoTherapy.* Australas Phys Eng Sci Med, 2011. **34**(3): p. 333-43.

11. Jacob, V., et al., *A planning comparison of dynamic IMRT for different collimator leaf thicknesses with helical tomotherapy and RapidArc for prostate and head and neck tumors.* Strahlenther Onkol, 2010. **186**(9): p. 502-10.

12. van Vulpen, M., et al., *Comparing step-and-shoot IMRT with dynamic helical tomotherapy IMRT plans for head-and-neck cancer.* Int J Radiat Oncol Biol Phys, 2005. **62**(5): p. 1535-9.

13. Luxton, G., S.L. Hancock, and A.L. Boyer, *Dosimetry and radiobiologic model comparison of IMRT and 3D conformal radiotherapy in treatment of carcinoma of the prostate.* Int J Radiat Oncol Biol Phys, 2004. **59**(1): p. 267-84.

14. Wolff, D., et al., *Volumetric modulated arc therapy (VMAT) vs. serial tomotherapy, step-and-shoot IMRT and 3D-conformal RT for treatment of prostate cancer.* Radiother Oncol, 2009. **93**(2): p. 226-33.

15. Fenoglietto, P., et al., *Persistently better treatment planning results of intensity-modulated (IMRT) over conformal radiotherapy (3D-CRT) in prostate cancer patients with significant variation of clinical target volume and/or organs-at-risk.* Radiother Oncol, 2008. **88**(1): p. 77-87.

16. Longobardi, B., et al., *Anatomical and clinical predictors of acute bowel toxicity in whole pelvis irradiation for prostate cancer with Tomotherapy.* Radiother Oncol, 2011. **101**(3): p. 460-4.

17. Adams, E.J., et al., *Clinical implementation of dynamic and step-and-shoot IMRT to treat prostate cancer with high risk of pelvic lymph node involvement.* Radiother Oncol, 2004. **70**(1): p. 1-10.

18. Bos, L.J., et al., *Comparison between manual and automatic segment generation in step-and-shoot IMRT of prostate cancer.* Medical Physics, 2004. **31**(1): p. 122-30.

19. Nicolini, G., A. Fogliata, and L. Cozzi, *IMRT with the sliding window: comparison of the static and dynamic methods. Dosimetric and spectral analysis.* Radiother Oncol, 2005. **75**(1): p. 112-9.

20. Cahlon, O., M. Hunt, and M.J. Zelefsky, *Intensity-modulated radiation therapy: supportive data for prostate cancer.* Semin Radiat Oncol, 2008. **18**(1): p. 48-57.

21. Ma, L., et al., *An optimized leaf-setting algorithm for beam intensity modulation using dynamic multileaf collimators.* Phys Med Biol, 1998. **43**(6): p. 1629-43.

22. Chanyavanich, V., et al., *Knowledge-based IMRT treatment planning for prostate cancer.* Med Phys, 2011. **38**(5): p. 2515-22.

23. Klein, S., et al., *elastix: a toolbox for intensity-based medical image registration.* IEEE Trans Med Imaging, 2010. **29**(1): p. 196-205.

24. Klein, S., M. Staring, and J.P.W. Pluim, *Evaluation of optimization methods for nonrigid medical image registration using mutual information and B-splines.* Ieee Transactions on Image Processing, 2007. **16**(12): p. 2879-2890.

25. Staring, M., et al., *Registration of cervical MRI using multifeature mutual information.* IEEE Trans Med Imaging, 2009. **28**(9): p. 1412-21.

26. Klein, S., et al., *Automatic segmentation of the prostate in 3D MR images by atlas matching using localized mutual information.* Medical Physics, 2008. **35**(4): p. 1407-1417.

27. van der Lijn, F., et al., *Cerebellum Segmentation in Mri Using Atlas Registration and Local Multi-Scale Image Descriptors.* 2009 Ieee International Symposium on Biomedical Imaging: From Nano to Macro, Vols 1 and 2, 2009: p. 221-224.

28. Yoon, M., et al., *A new homogeneity index based on statistical analysis of the dose-volume histogram.* J Appl Clin Med Phys, 2007. **8**(2): p. 9-17.

29. Takam, R., et al., *Assessment of normal tissue complications following prostate cancer irradiation: comparison of radiation treatment modalities using NTCP models.* Med Phys, 2010. **37**(9): p. 5126-37.

30. Hamilton, M.J., *Wilcoxon Signed Rank Test*, U.o.N. Mexico, Editor 2004.

31. Drzymala, R.E., et al., *Dose-volume histograms.* Int J Radiat Oncol Biol Phys, 1991. **21**(1): p. 71-8.